Flooding Management using Hybrid Model Predictive Control: Application to the Spanish Ebro River

J. Romera[†], C. Ocampo-Martinez[†,‡,*], V. Puig[†,‡] and J. Quevedo[†]

[†]Automatic Control Department, Technical University of Catalonia
Rambla Sant Nebridi, 10, 08222 Terrassa, Spain
[‡]Institut de Robòtica i Informàtica Industrial (CSIC-UPC)
Llorens i Artigas, 4-6, 08028 Barcelona, Spain

Abstract

In this paper, the problem of flooding management using hybrid model predictive control is presented and applied to the Ebro River in Spain. The Ebro river presents flooding episodes in the city of Zaragoza during spring when snow melts in the Pyrenees. To avoid flooding in living areas, some lands outside the city are prepared to be flooded. This paper presents a control approach to determine and fix the level of flooding in pre-established zones by controlling side gates that determine the water input to the land to be flooded. Finally, several scenarios are used to validate the performance of the proposed approach.

Keywords: Water systems, rivers, simulation, predictive control, tele-control systems

1 Introduction

River flooding are extreme episodes necessary for the adequate functioning of rivers and their associated ecosystems. In order to coexist in harmony with flooding, their prevention and control is an important topic in the management of those systems. The reason is due to the fact that river flooding may cause large economic losses when they are not appropriately managed.

The most common and utilised technique for flooding management is based on operating rules, which merge heuristic approaches, operator judgement and experience. While these approaches may be adequate in most of the cases, the best operational policies may be quite complex for large-scale interconnected systems. On the other hand, decision support systems (DSS), which are based on mathematical models of the system operation and optimal control techniques, provide useful guidance for efficient management of flooding in rivers [5].

Model Predictive Control (MPC) is a technique that allows to take into account physical and operational constraints, multivariable and large-scale features, transport delays, disturbance forecasting and multi-objective operational goals [14]. The optimal strategies are computed by optimising a mathematical function describing the operational goals in a given time horizon and using a representative model of the system dynamics, as well as disturbance forecasts, if available. Thus, MPC is a suitable technique to deal with the flooding management in rivers because of the multivariate and complex dynamics of those systems, which make the control

*Corresponding author. Tel: +34 93 401 5752. Fax: +34 93 401 5750. E-mail: cocampo@iri.upc.edu

problem challenging. Moreover, since rivers present important transport delays, MPC allows to compute optimal control strategies ahead in time for all the control elements of the river system.

In most water systems, the regulated elements, namely pumps, gates and retention devices, are typically controlled locally, i.e., they are controlled by a remote station according to the measurements of sensors connected only to that station. However, a global real-time control (RTC) system requires the use of an operational model of the system dynamics in order to compute, ahead of time, optimal control strategies for the actuators based on the current state of the system provided by supervisory control and data acquisition (SCADA) sensors, the current disturbance measurements and appropriate disturbance predictions. The computation procedure of an optimal global control law should take into account all the physical and operational constraints of the dynamical system to produce set-points that allows to achieve the given control objectives. Within this global control framework, MPC has shown to be a suitable strategy to implement global RTC of water systems since it has important features to deal with complex behaviours and features such as big delays compensation, the use of physical constraints, relatively simple for people without deep knowledge of control, multi-variable systems handling, among others. MPC, as global control law, determines the optimal set-points for local controllers already existing in the field.

Reviewing the literature, MPC has already been proposed for flooding management by several authors. In [24], a multiple-model MPC scheme for a large drainage canal system in the Netherlands is proposed. This control approach allows to deal with uncertainty in the expected inflow by minimizing an objective function in which the risk of damage is used by applying different scenarios to multiple identical models. On the other hand, in [3] a non-linear MPC scheme to address the flooding problem of the Demer river in Belgium is presented. The proposed MPC approach is based on a new semi-condensed optimization procedure combined with a line search approach.

The use of optimal/predictive control techniques for flooding management requires the development of control-oriented dynamic models to represent open-channel systems and associated hydraulic structures (e.g., gates, weirs, dams), which might have non-linear responses to control actions. On the other hand, the storage (tanks and dams) and control elements (gates, valves and pumps), with a pre-determined operational range, lead to the inclusion of constraints besides the model formulation. Moreover, there exist several inherent phenomena and/or elements in the system that result in distinct behaviour depending on its state. These discontinuous behaviours can not be neglected nor can be modelled by a pure linear model. To take into account these behaviours, a control-oriented model methodology that allows considering and incorporating flooding and other logical dynamics in some of the system elements is needed. In previous works reported by the authors, a hybrid modelling approach based on the Mixed Logical Dynamical (MLD) form, introduced in [2], was used to model hybrid elements in sewer networks (see [19] for further details).

However, the inclusion of those discontinuous behaviours in the MPC problem increases the computation time of the control law [18]. Therefore, some relaxation should be thought in the modelling approach such that it can be considered within the RTC of river systems. Thus, one of the contributions of this paper is to propose a control-oriented modelling approach that takes into account the continuous/discrete dynamic behaviours that can be used when performing an MPC-based RTC scheme for river systems. The proposed approach models the hybrid behaviours by using piece-wise linear (PWL) functions, following the ideas proposed in [22]. The aim of this modelling approach, namely in the sequel PWLF model, is to reduce the complexity of the MPC problem by avoiding the logical variables introduced by a mathematical system representation such as MLD form. The idea behind the PWLF modelling approach consists in having a description of the network using functions that, despite their discontinuous nature, are

considered as quasi-convex [4] and hence the optimization problems associated to the non-linear MPC strategy used for RTC of the river system. In this way, the resulting optimization problems do not include integer variables, which allows saving computation time.

As the case study, this paper presents the flooding management problem in the basin of the Ebro river in Spain. In the past, the Ebro basin experienced several flooding. In order to reduce the associated hazard in a given area, the local water administration usually set up several flooding-controlled areas for being able to store the excessive water volume during periods of extreme rainfall. To control the flows from/to the flooding zones, hydraulic control structures have been put in place. Through these actions, it is planned to have a significant reduction of the flooding risk in the basin. Simulations of these past events in a hydrodynamic river model will show that flooding can be further reduced if the hydraulic structures are controlled using MPC to decide the optimal time to open/close the gates. Notice that the formulation of both the system model and the associated MPC strategy are deeply related to the placement of the gates, here called *side gates*. This feature makes the problem more challenging due to its special structure.

The paper is organised as follows. In Section 2 the Ebro river case study is introduced. Section 3 describes the control-oriented modelling principles used as well as their application to the case study. Section 4 presents the Hybrid MPC (HMPC) strategy used in this paper to manage flooding in the Ebro river case study. The main simulation results of the closed-loop scheme proposed here are collected and discussed in Section 5, while in Section 6 the most relevant conclusions are drawn.

2 The Ebro River Case Study

The Ebro River has the largest Mediterranean basin in the Iberian Peninsula (with a 930 km long channel and 85000 km^2 basin) and the third one by surface among those of the Mediterranean Sea (see Figure 1). Its average contribution, of about 14 km^3 per year, represents almost 4% of the total Mediterranean basin contributions. The Middle Ebro River presents a meandering channel with a very low slope. The average width of the floodplain is 3.2 km, having a maximum width of 6 km. The mean sinuosity index is 1.505 and the average channel slope is 0.67 m/km. Along the river channel a progressive loss of specific discharge is recorded. In the Middle Ebro River stands out the remarkable increase of discharge contributed from the Aragon River basin, which drains the Western Pyrenees. Thus, flooding processes are common in this river reach, but the combination among decrease of discharges, dam construction and expansion and reinforcement of defences have created an unusually quiet period as regards flooding events during the last quarter of the previous century. Nevertheless, with the turn of the century, it seems that the Middle Ebro River has entered into new dynamics, with bigger and more frequent flooding. This fact has made that its seasonal nature has changed [7]. Important flooding episodes appear around the city of Zaragoza in spring, given when snow melts in the Pyrenees or due to the excessive precipitation and surface runoff, being them the cause of extensive damage, loss of property and human suffering. To avoid flooding in living areas, some lands outside the city are prepared to be flooded. These flooding areas are surrounded by levee breaches and connected to the river by controlled side gates.

Figure 2 presents three inundation lateral areas located along the river. The flooding going in and out to these areas can be controlled using side gates. The idea is the following: when a flooding episode starts, side gates might be open to start filling the flooding zones and get closed when they are full or it is not possible to keep on filling. On the other hand, when the flow at the control point downstream is going down below some pre-established safety flow, side gates should

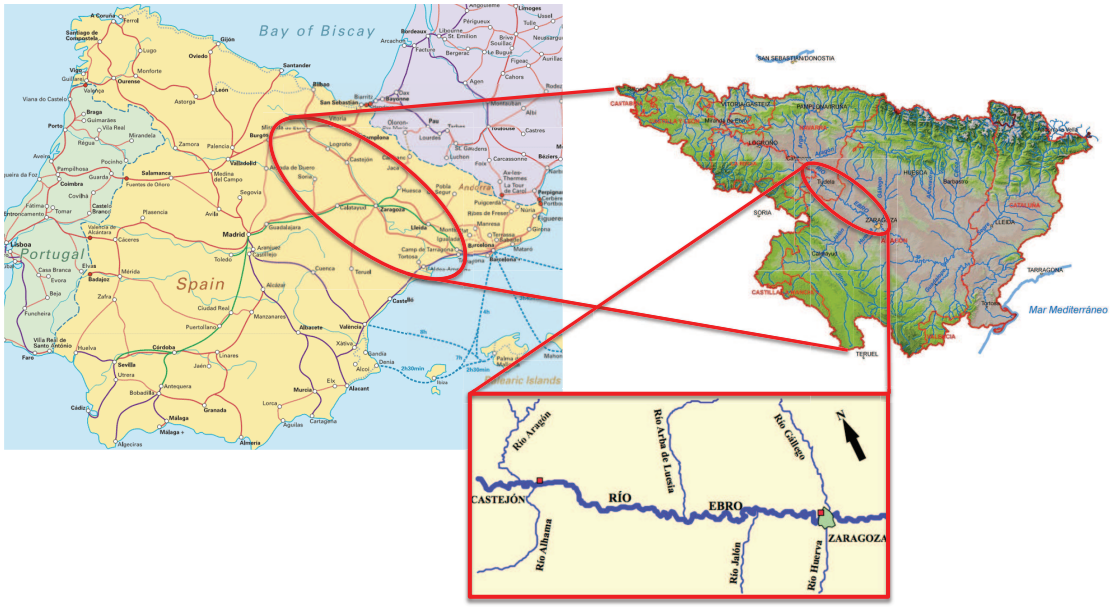

Figure 1: Ebro River Basin and detail of the case-study place

be opened again to start emptying the flooding zones. Thus, there are two desired management objectives: the first consists in limiting the maximum flow at the control point under the safety flow, and the second one consists in keeping the flooding zones as empty as possible in order to empty them at the end of the flooding scenario. All the river long and the flooding zones are separated by vertical walls (levees) of 8 m height except at the gate locations (see Figure 3).

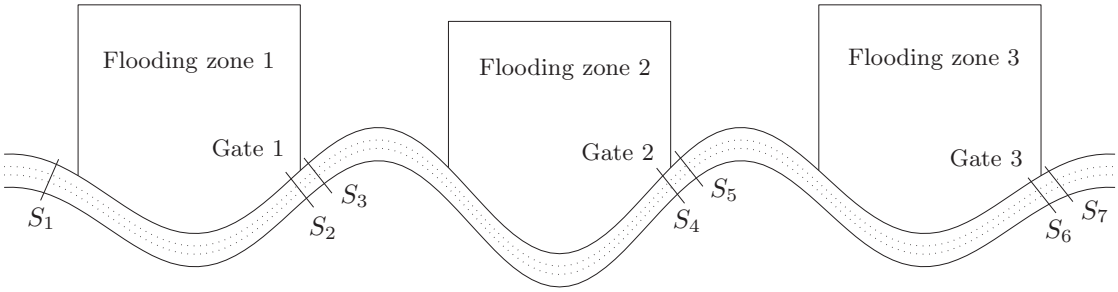

Figure 2: Scheme of the considered river stretch and disposition of the flooding zones and side gates

Side gates allow bidirectional water flow, which depends on the water level at each side of the gate. In order to test the proposed hybrid predictive controller, a high-fidelity simulator (HFS), based on the well-known Saint-Venant equations describing sub-critical, critical and super-critical flow, has been used [17]. Additionally, these equations allow reproducing effects such as inertial phenomena, backwater effects and the attenuation of wave flow along the time and space. The implemented hydraulic model is based on the 2-D Saint-Venant equations for the description of continuity and momentum conservation [9]. The numerical method implemented is based on a four-point implicit finite difference scheme, where the partial differential equations are replaced

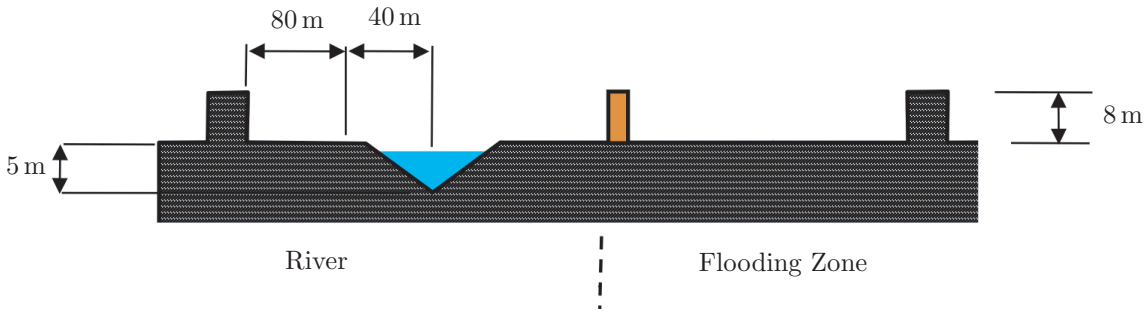

Figure 3: River cross section at a side gate location

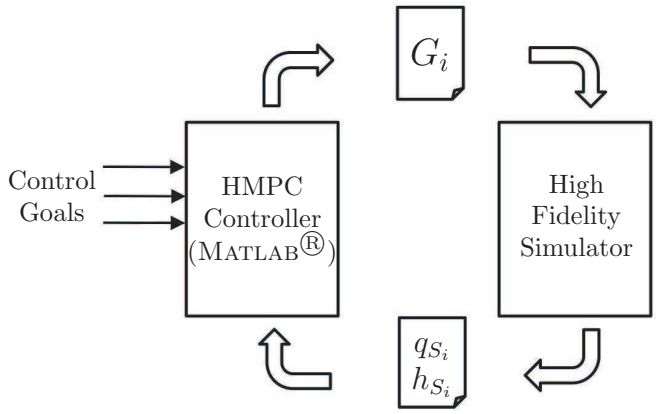

Figure 4: Scheme of the closed loop for the simulation scenarios

by the evaluation of functions at discrete points. For each interaction step, a sparse matrix is computed [16, 6]. For more details about the 2D HFS considered in this paper, see [16, 17, 9] and references therein.

In order to perform the closed-loop control taking into account the HFS, the procedure graphically depicted in Figure 4 is followed. There, measurements of flow q_{S_i} and level h_{S_i} for each river reach are taken from the HFS and brought to the HMPC controller. This controller computes the values for side-gates opening $G_{0,i}$ according to the preestablished control goals, which are collected in the corresponding cost function described later.

3 Control-oriented Modelling

3.1 River reach models

One of the most important stages on the design of RTC schemes for open-flow canals, in such a case of using a model-based control technique, lies on the modelling task. This fact is given since the performance of model-based control techniques relies on the model quality. Thus, in order to design an MPC-based RTC scheme with a proper performance, a system model with accuracy enough should be used but keeping complexity manageable.

Water flow in rivers is open canal. The Saint-Venant equations, based on physical principles

of mass conservation and energy, allow the accurate description of the open-channel flow and therefore also allow having a detailed nonlinear description of the system behaviour. Associated to this concept is the volumetric flow rate, which can be thought as the mean velocity of the water flow through a given cross-section, multiplied by its cross-sectional area. Mean velocity can be approximated through the use of the Law of the Wall [1, 15]. In general, velocity increases with the depth (or hydraulic radius) and slope of the river canal, while the cross-sectional area scales with the depth and the width: the double counting of depth shows the importance of this variable in determining the discharge through the canal.

Notice that models based on Saint-Venant equations describe the system behaviour in high detail. However, such a level of detail is not manageable for RTC implementation because of the complexity and the high computational cost of combining those equations with the MPC strategy. Alternatively, several conceptual modelling techniques that deal with RTC of rivers have been proposed: Hayami model [11, 12], Muskingum model [8], integrator delay zero (IDZ) model [10] or black-box models identified using parameter estimation [25].

In this paper and according to [10], a single reach canal dynamics can be approximated by using the IDZ model given by

$$H_{dns}(s) = G_{ups}(s)Q_{ups}(s) + G_{dns}(s)Q_{dns}(s), \tag{1}$$

where s denotes the Laplace variable, $H_{dns}(s)$ is the water level (in m) at the control point, and $Q_{ups}(s)$, $Q_{dsn}(s)$ are the upstream and downstream flows (in m^3/s), respectively. Moreover, $G_{ups}(s) = e^{-\tau_d s}/A_d s$ and $G_{dns}(s) = -1/A_d s$ with τ_d being the downstream transport delay (in seconds) and A_d the downstream backwater area (in cubic meters).

Taking into account the linearised relation between Q_{dns} and H_{dns} in the control point, the following relation can be established:

$$Q_{dns}(s) = \beta H_{dns}(s), \tag{2}$$

where β is a constant that should be estimated experimentally. Combining (1) and (2), the following first order plus time delay (FOPTD) model is obtained:

$$G(s) = \frac{Q_{dns}(s)}{Q_{ups}(s)} = \frac{Ke^{-\tau_d s}}{Ts+1}, \tag{3}$$

with $K = 1$ and $T = A_d/\beta$. This model can be represented in discrete-time using a zero-order hold to model analog-to-digital (and viceversa) converters and a sampling time Δt (in s), as follows:

$$G_d(z) = \frac{Q_{dns}(z)}{Q_{ups}(z)} = \frac{b_0 z^{-(\delta+1)}}{1 - a_1 z^{-1}}, \tag{4}$$

where $\delta = \lfloor \tau_d/\Delta t \rfloor$, $b_0 = 1 - a_1$, and $a_1 = e^{-\frac{\Delta t}{T}}$. The symbol $\lfloor\ \rfloor$ denotes the floor rounding. Alternatively, it can be written as a difference equation as

$$q_{dns}(k+1) = a_1 q_{dns}(k) + b_0 u(k-\delta). \tag{5}$$

Using the control-oriented modelling methodology presented, the Ebro river reach presented in Figure 2 can be represented by the block diagram in Figure 5.

Each river reach has been identified experimentally using the IDZ model structure proposed by Litrico [10] and the least-square parameter estimation approach [13] by means of the System Identification Toolbox for MATLAB®, leading to a set of discrete transfer functions $G_i(z)$, for

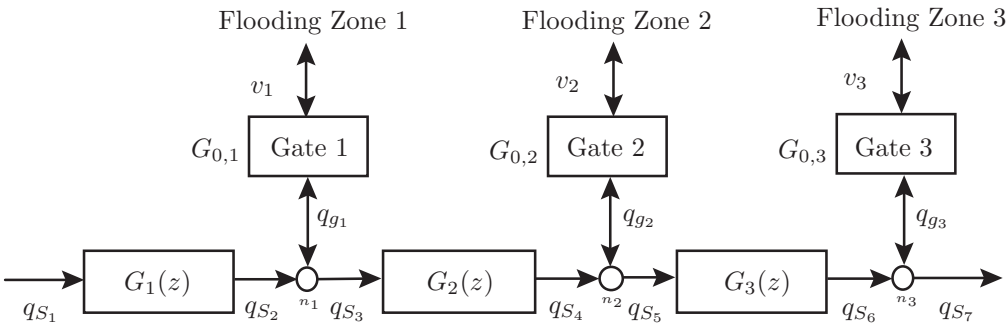

Figure 5: Block diagram of the Ebro river reach

$i \in \{1, 2, 3\}$. For the case study of this article and performing the proper adjustments of these discrete transfer functions, yields

$$G_1(z) = \frac{0.1432z^{-8}}{1 - 0.8547z^{-1}}, \qquad G_2(z) = \frac{0.09515z^{-8}}{1 - 0.9049z^{-1}}, \quad \text{and} \quad G_3(z) = \frac{0.1247z^{-8}}{1 - 0.8761z^{-1}}. \tag{6}$$

Figure 6 shows the degree of adjustment of each discrete transfer function $G_i(z)$ for each of the three river reaches provided by the `compare` command of the System Identification Toolbox for MATLAB®. Notice that the comparison has been done with each river reach flow $q_{S_p}(k)$, for $p \in \{2, 4, 6\}$, given by the HFS.

However, even if the real measurements are flows, the flow from/to river to/from flooding zones is determined by the water levels at both sides of the side gates (see Section 3.3). Therefore, a proper conversion from flow $q_{S_p}(k)$ to level $h_{S_p}(k)$, for $p \in \{2, 4, 6\}$, should be performed. Given that the HFS provides with the flow and level at each measuring point S_p, a curve fitting procedure has been performed by using a set of data obtained when simulating with a generic hydrogram, namely $q_{S_1}(k)$, as the input of the system. Hence, the following polynomials have been obtained:

$$h_{S_m}(k) = a_{(m,2)} q_{S_m}(k)^2 + a_{(m,1)}\, q_{S_m}(k) + a_{(m,0)}, \tag{7}$$

where $m \in \{2, 4, 6\}$ and the value of the coefficients $a_{(m,2)}$, $a_{(m,1)}$ and $a_{(m,0)}$ are collected in Table 1 in the Appendix. Figure 7 presents the curves of the flow/level relation at S_2, S_4 and S_6 and the corresponding polynomial including its percentage of fitting.

Additionally to those dynamics, the river model presented here considers three static relations at the nodes n_i, $i \in \{1, 2, 3\}$ (see Figure 5), which are written as

$$q_{S_3}(k) = q_{S_2}(k) + q_{g_1}(k), \tag{8a}$$
$$q_{S_5}(k) = q_{S_4}(k) + q_{g_2}(k), \tag{8b}$$
$$q_{S_7}(k) = q_{S_6}(k) + q_{g_3}(k). \tag{8c}$$

Notice that flows $q_{S_p}(k)$, for $p \in \{1, \ldots, 7\}$, are only defined in one direction, while $q_{g_i}(k)$ are bidirectional. Then, in these latter flows their sign (plus/minus) in (8) are given by their direction.

3.2 Flooding Zone Model

In order to compute the water level within the flooding zones, i.e., $h_{fz,i}(k)$, for $i = \{1, 2, 3\}$, the behaviour of the corresponding water volume, namely $v_i(k)$, should be expressed and properly

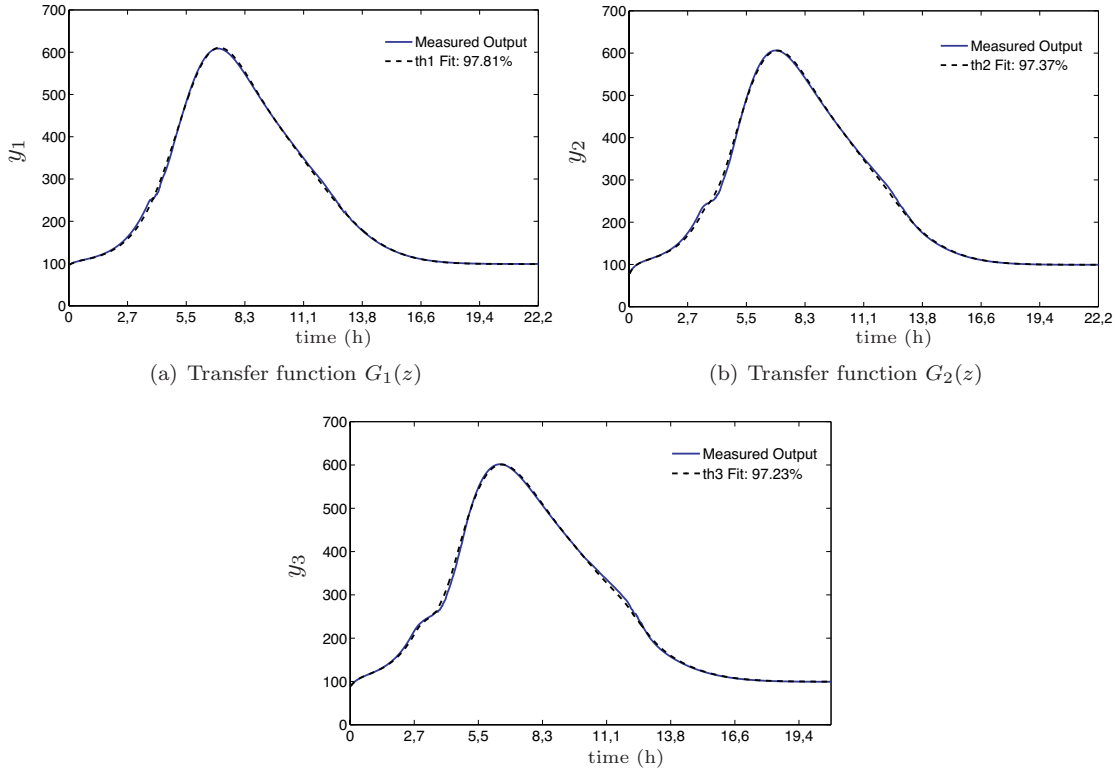

(a) Transfer function $G_1(z)$

(b) Transfer function $G_2(z)$

(c) Transfer function $G_3(z)$

Figure 6: Transfer function adjustments

evolved through the expression

$$v_i(k+1) = v_i(k) + \Delta t\, q_{g_i}(k), \tag{9}$$

where Δt is the sampling time, which is 100 s for this case study. Thus, the evolution of the levels inside the flooding zone $h_{fz,i}(k)$ is obtained by using a set of polynomials such as the case of the flow and level in the model of side gates. Here, polynomials relate $v_i(k)$ with $h_{fz,i}(k)$ in the following way:

$$v_i(k) = b_{(i,5)}h_{fz,i}(k)^5 + b_{(i,4)}h_{fz,i}(k)^4 + b_{(i,3)}h_{fz,i}(k)^3 + b_{(i,2)}h_{fz,i}(k)^2 + b_{(i,1)}h_{fz,i}(k) + b_{(i,0)}, \tag{10}$$

where $i = \{1, 2, 3\}$ and the value of the coefficients $b_{(i,j)}$, for $j \in \{0, \ldots, 5\}$ are collected in Table 1 in the Appendix. Figure 8 presents the curves of the volume/level relation at the corresponding flooding zone and its polynomial with a percentage of fitting of about 98%.

3.3 Hybrid Behaviours

In the considered case study, side gates in charge of filling/emptying the flooding zones are the elements responsible of adding the hybrid feature to the mathematical model proposed here. Their description and the fact of considering their control induce an added complexity not only to the modelling problem but also to the MPC problem.

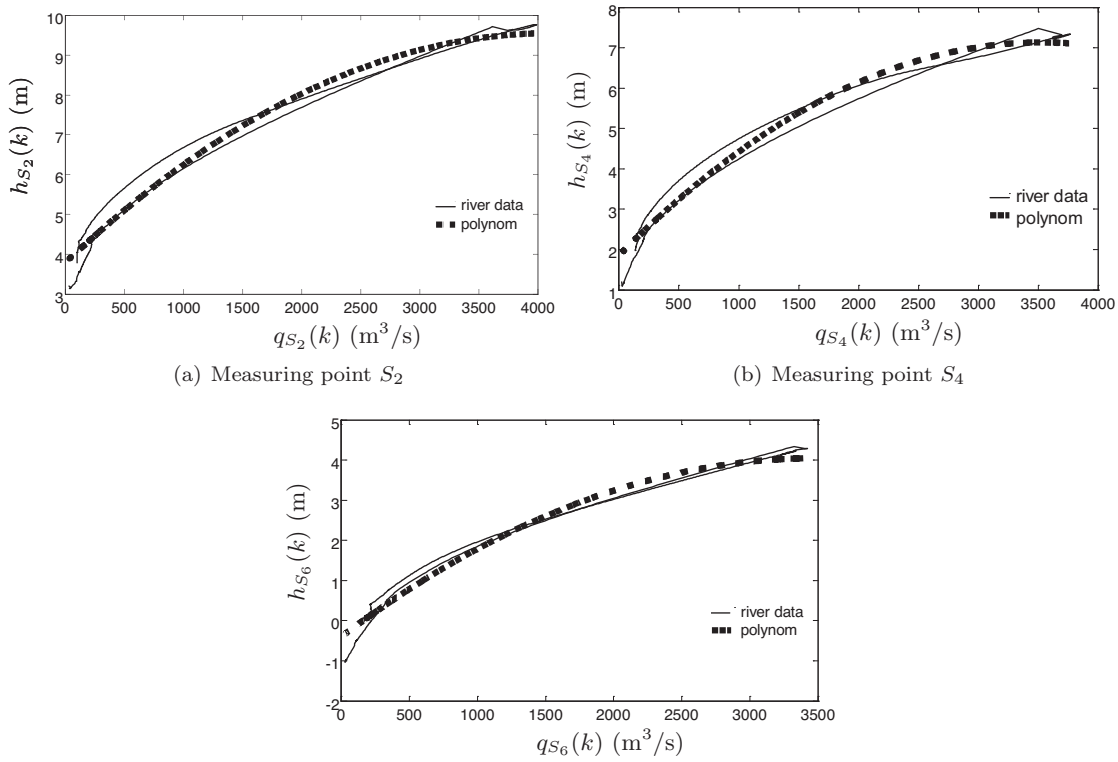

(a) Measuring point S_2

(b) Measuring point S_4

(c) Measuring point S_6

Figure 7: Flow/Level adjustments

The mathematical operational model of the side gates can be derived taking into account that, depending on the water level at the river side or inside the flooding zone, the controller might open or close the side gate to fill/empty the zone. Hence, the side gate model depends on water levels at both sides, as illustrated in Figure 9. In this figure, $d_j(k) \triangleq h_j(k) + z_j$, where $d_j(k)$ corresponds to the absolute level of water referenced to a point downstream, $h_j(k)$ is the relative level of water, and z_j are the heights of the bottom part of the side gate with respect to a given reference point.

The flow through a side gate i can be computed as

$$q_{g_i}(k) = \begin{cases} G_{0,i}(k)K_1\sqrt{d_{fz,i}(k) - d_{r,i}(k)} & \text{if} \quad d_{fz,i}(k) > d_{r,i}(k) \quad \text{and} \quad d_{r,i}(k) > \lambda_i(k), \\ G_{0,i}(k)K_2\sqrt{d_{fz,i}(k) - z_{fz,i}} & \text{if} \quad d_{fz,i}(k) > d_{r,i}(k) \quad \text{and} \quad d_{r,i}(k) \leq \lambda_i(k), \\ G_{0,i}(k)K_1\sqrt{d_{r,i}(k) - d_{fz,i}(k)} & \text{if} \quad d_{fz,i}(k) \leq d_{r,i}(k) \quad \text{and} \quad d_{fz,i}(k) > \lambda_i(k), \\ G_{0,i}(k)K_2\sqrt{d_{r,i}(k) - z_{fz,i}} & \text{if} \quad d_{fz,i}(k) \leq d_{r,i}(k) \quad \text{and} \quad d_{fz,i}(k) \leq \lambda_i(k), \end{cases} \tag{11}$$

for $i = 1, 2, 3$, where $G_{0,i}(k)$ is the side gate opening and $\lambda_i(k) = z_{fz,i} + G_{0,i}(k)$. Constants K_1 and K_2 are related to the gate physical model. The values of the physical parameters and constants are given in Table 1 in the Appendix.

In this paper, the hybrid modelling framework based on PWL functions is used to model such behaviours. The PWLF modelling methodology, proposed in [20], consists in using continuous and monotonic functions to represent expressions that contain logical conditions, which describe

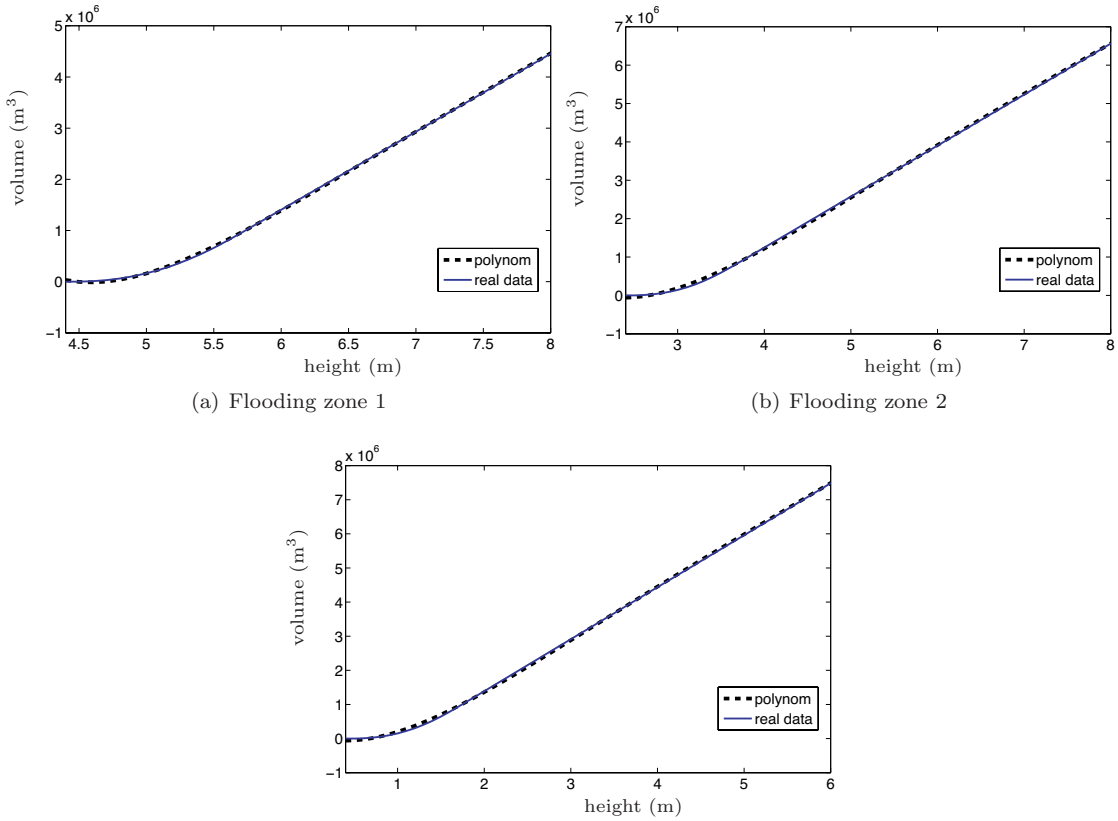

(a) Flooding zone 1

(b) Flooding zone 2

(c) Flooding zone 3

Figure 8: Curves flow/height and volume/height

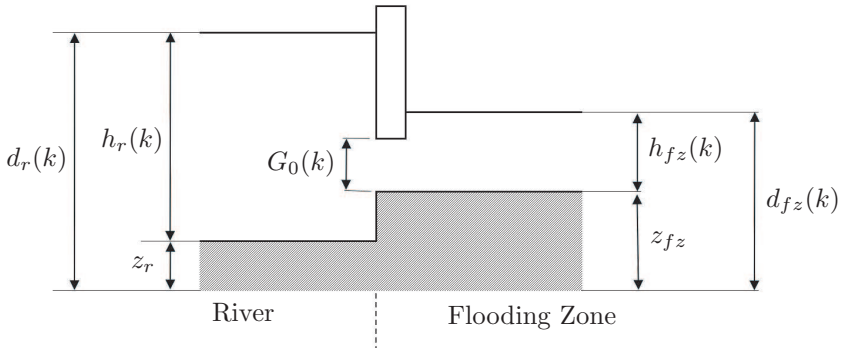

Figure 9: Side gate scheme and its main parameters and variables associated

the nonlinear discontinuous behaviours. Those PWL functions are monotonic and continuous, leading to a quasi-convex optimization problem when formulating the MPC problem. According to [4], the global optimal solution of quasi-convex problems can be obtained by using non-linear programming algorithms. This fact represents an advantage with respect to the mixed-integer linear program that is obtained when using a pure hybrid approach based on MLD (or PWA)

approaches, since mixed-integer linear programming has an exponential complexity while non-linear programming only polynomial.

More precisely, the motivation for performing a PWLF model from the application case presented in this paper rather than other well-accepted hybrid model frameworks for MPC based on MLD modelling approach is discussed as follows. In previous works reported by the authors sewage system management applications [21], stating an MLD model with 12 continuous states and prediction horizon $H_p = 6$, the computation time needed for obtaining a control signal from the hybrid MPC controller is bigger than the corresponding sampling time (for those cases 300 s). In the current flooding control application, the sampling time used is smaller (100 s), the prediction horizon $H_p = 42$ is longer and the state space representation in MLD form would imply 24 states since there are three river reaches modelled with a first-order model plus a delay of eight samples. Moreover, side gate models are non-linear, therefore to use an MLD model, a linearisation of such non-linear models would imply to introduce an important number of binary variables that increase further the computation time required. For all these reasons, it makes no sense to consider MLD models (and their associated predictive control design) with the Ebro case study.

The PWL functions used to model the discontinuous behaviours that appear in the side gate operation model (11) are defined as *saturation* of a variable x in a value M (i.e., $sat(x, M)$), and *dead zone* of the same variable x starting in a value M (i.e., $dzn(x, M)$). Those functions are monotonic and continuous and might lead to a quasi-convex optimisation problem when formulating the MPC problem. According to [4], the global optimal solution of quasi-convex optimisation problems can be obtained by using a bisection method, which is logarithmic in time. This fact represents an advantage with respect to the mixed-integer linear problems resulting when using a pure hybrid approach based on MLD forms or piece-wise affine (PWA) approaches. This type of models induces an exponential complexity given by the handling of Boolean variables and the discrete optimization required. The continuous and monotonic functions related to the modelling approach used in this paper are defined as follows:

- Saturation function, defined as

$$\mathrm{sat}(x, M) = \begin{cases} x & \text{if} \quad 0 \leq x \leq M, \\ M & \text{if} \quad x > M, \\ 0 & \text{if} \quad x < 0. \end{cases} \tag{12}$$

- Dead-zone function, defined as

$$\mathrm{dzn}(x, M) = \begin{cases} x - M & \text{if} \quad x \geq M, \\ 0 & \text{if} \quad x < M. \end{cases} \tag{13}$$

In order to express (11) using PWL functions, the following definitions related to the *if* conditions are stated:

$$\alpha_{1,i}(k) = \frac{\mathrm{dzn}(\tilde{d}_i(k), 0)}{\tilde{d}_i(k) + \epsilon}, \qquad \alpha_{2,i}(k) = \frac{\mathrm{dzn}(-\tilde{d}_i(k), 0)}{-\tilde{d}_i(k) + \epsilon}, \tag{14a}$$

$$\beta_{1,i}(k) = \frac{\mathrm{dzn}(d_{r,i}(k) - \lambda_i(k), 0)}{d_{r,i}(k) - \lambda_i(k) + \epsilon}, \qquad \beta_{2,i}(k) = \frac{\mathrm{dzn}(-d_{r,i}(k) + \lambda_i(k), 0)}{-d_{r,i}(k) + \lambda_i(k) + \epsilon}, \tag{14b}$$

$$\gamma_{1,i}(k) = \frac{\mathrm{dzn}(d_{fz,i}(k) - \lambda_i(k), 0)}{d_{fz,i}(k) - \lambda_i(k) + \epsilon}, \qquad \gamma_{2,i}(k) = \frac{\mathrm{dzn}(-d_{fz,i}(k) + \lambda_i(k), 0)}{-d_{fz,i}(k) + \lambda_i(k) + \epsilon}, \tag{14c}$$

where $\tilde{d}_i(k) = d_{fz,i}(k) - d_{r,i}(k)$ and $\epsilon > 0$ is a very small positive constant used to avoid numerical problems given by the possible division by zero. Hence, the expression for the flow through the i-th gate is given by

$$q_{g_i}(k) = \rho\, G_{0,i}(k)\, \left[\, \alpha_{1,i}(k)\, q_{a,i}(k) - \alpha_{2,i}(k)\, q_{b,i}(k) \,\right], \tag{15}$$

where

$$q_{a,i}(k) = K_1 \beta_{1,i}(k) \sqrt{\tilde{d}(k)} + K_2 \beta_{2,i}(k) \sqrt{d_{fz,i}(k) - z_{fz,i}}, \tag{16a}$$

$$q_{b,i}(k) = K_1 \gamma_{1,i}(k) \sqrt{-\tilde{d}(k)} + K_2 \gamma_{2,i}(k) \sqrt{d_{r,i}(k) - z_{fz,i}}, \tag{16b}$$

and ρ is the side gate width.

4 Hybrid Predictive Control Strategy

4.1 Fundamentals

By definition, the HMPC problem using the PWLF-based modelling approach presented in [20] can be formulated as a non-linear MPC (NMPC) problem since the model of the system to be controlled is finally expressed in a general form as

$$x(k+1) = f(x(k), u(k)), \tag{17}$$

being $x_k \in \mathbb{X} \subseteq \mathbb{R}^n$ the mapping of states and $u_k \in \mathbb{U} \subseteq \mathbb{R}^m$ the control signals, where $f : \mathbb{R}^n \times \mathbb{R}^m \to \mathbb{R}^n$ is an arbitrary system state function and $k \in \mathbb{Z}_+$. Then, the MPC is based on the solution of the open-loop optimisation problem (OOP)

$$\min_{\{u(k)\}_{i=0}^{H_p-1}} \sum_{j=0}^{H_p-1} J\left(u(k+j|k), x(k+j+1|k)\right), \tag{18a}$$

subject to

$$H_{iq}^{\mathrm{u}} u(k+j) \leq b_{iq}^{\mathrm{u}}, \tag{18b}$$

$$E_{iq} x(k+j) + H_{iq} u(k+j) \leq b_{iq}, \tag{18c}$$

$$H_{eq}^{\mathrm{u}} u(k+j) = b_{eq}^{\mathrm{u}}, \tag{18d}$$

$$E_{eq} x(k+j) + H_{eq} u(k+j) = b_{eq}, \tag{18e}$$

$\forall\, j \in [0, H_p - 1]$, where $J(\cdot)$ is the cost function, H_p denotes the *prediction horizon* or *output horizon*, and E_{iq}, E_{eqe}, H_{iq}, H_{eq}, H_{iq}^{u}, H_{eq}^{u}, b_{iq}, b_{eq}, b_{iq}^{u}, and b_{eq}^{u} are matrices with suitable dimensions. In (18a), $x(k+j|k)$ denotes the prediction of the state at time $k+j$ performed at k, starting from $x(0|k) = x(k)$. When $H_p = \infty$, the OOP is called the *infinite horizon problem*; when $H_p \neq \infty$, the OOP is called the *finite horizon problem*. Constraints employed to guarantee the stability of the system in a closed loop would be added in (18b)–(18e). In particular, constraints (18d)–(18e) are related to elements with static dynamics, where an equality condition must hold.

The optimal solution of the OOP (18) is given by the sequence

$$\mathbf{U_k}^* \triangleq \left(u(0|k)^*, u(1|k)^*, \ldots, u(H_p - 1|k)^*\right), \tag{19}$$

and then the receding horizon philosophy sets

$$u_{\mathrm{MPC}}(x(k)) \triangleq u(0|k)^*, \tag{20}$$

and disregards the computed inputs from $k = 1$ to $k = H_p - 1$, with the whole process repeated at the next time instant $k \in \mathbb{Z}_+$. Expression (20) is known in the MPC literature as *the MPC law* [14].

4.2 Management Criteria (Control Objectives)

In the Ebro case study, three control objectives have been considered. The most important objective of this control problem is to minimize the effects of the flooding in downstream populations. Therefore, the main goal is to limit the maximum flow at the output of the system, denoted as S_7 in Figure 2, following the expression

$$J_1(k) = \begin{cases} q_{S_7}(k) - q_d & \text{if} \quad q_{S_7}(k) \geq q_d, \\ 0 & \text{if} \quad q_{S_7}(k) < q_d, \end{cases} \tag{21}$$

where $q_{S_7}(k)$ is the flow at the output of the system and q_d is the desired maximum flow (reference). Then, the expression of this objective using PWL functions is written as

$$J_1(k) = \mathrm{dzn}(q_{S_7}(k) - q_d, 0). \tag{22}$$

Similarly, this objective aims at preserving, as much as possible, the flooding zones from the bad effects of flooding. Following this idea, a second objective is defined. Once the flooding has passed, this second goal would force the emptying of the flooding zones to evacuate the stored amount of water in a safety way. The expression for this objective can be written as

$$J_2(k) = \begin{cases} 0 & \text{if} \quad q_{S_7}(k) \geq q_d, \\ \sum_{i=1}^{3} v_i(k) & \text{if} \quad q_{S_7}(k) < q_d. \end{cases} \tag{23}$$

Then, the expression of this objective using PWL functions is

$$J_2(k) = \frac{\mathrm{dzn}(q_d - q_{S_7}(k), 0)}{q_d - q_{S_7}(k) + \epsilon} \sum_{i=1}^{3} v_i(k). \tag{24}$$

Moreover, to obtain a smoothing effect in the operation of the side gates, the control signal variation between consecutive time intervals is penalised. Hence, this penalisation is achieved by minimizing

$$J_3(k) = \sum_{i=1}^{3} \Delta q_{g_i}(k)^2. \tag{25}$$

Finally, the multi-objective performance function $\mathcal{J}(k)$ that gathers the aforementioned control objectives can be written as

$$\mathcal{J}(k) = \omega_1 J_1(k) + \omega_2 J_2(k) + \omega_3 J_3(k), \tag{26}$$

where ω_i are the weighting factors used in the normalisation and prioritisation of the different control objectives. Each objective of (26) has been normalized taking into account the operating range of each variable. The normalized objectives and weights are denoted by $\bar{J}_i$ and $\bar{\omega}_i$, respectively. The weight factors have been adjusted taking into account that Objectives J_1 and J_2 do

not apply simultaneously. In fact, they are exclusive since the Objective J_1 applies when flow at the output of the system is above the flooding limit. On the other hand, Objective J_2 applies when this flow is below the flooding limit. This is why the weight for both objectives is being set to one. Therefore, the real trade off appears between Objectives J_1 and J_3 in the filling phase, and between Objectives J_2 and J_3 in the emptying phase. The value of the weight related to Objective J_3 is set smaller compared to the weight associated to Objective J_1 but large enough to smooth the operation of side gates. At this point, particular weight values have been selected by standard trial-and-error procedures. Thus, the final values of the normalized weights have been set as $\bar{\omega}_1 = 1$, $\bar{\omega}_2 = 1$ and $\bar{\omega}_3 = 0.1$. Other methodologies for tuning MPC controllers in water systems may be taken into account (see [23] and references therein), but this topic is out of the scope of this paper.

4.3 Predictive Controller Design

Considering the case study presented in this paper, the HMPC design is based on the solution of a OOP such as in (18), where the cost function (18a) is written as

$$\min_{\{G_{0,i}(k+j)\}_{j=\delta}^{H_p-1}} \sum_{j=\delta}^{H_p-1} \sum_{i=1}^{3} \bar{\omega}_i \, \bar{J}_i(k+j|k), \tag{27}$$

subject to the constraints given in (7), (8), (15), (9), and the physical constraints

$$G_{0,i}^{\min} \leq G_{0,i}(k) \leq G_{0,i}^{\max}, \tag{28a}$$

$$0 \leq v_i(k) \leq v_i^{\max}, \tag{28b}$$

$$q_{S_i}(k) \geq 0, \tag{28c}$$

for all $k \in H_p$ and $i = 1, 2, 3$. Notice that the cost function considers the value of the objectives J_i in the time horizon H_p starting from the time instant δ to consider the transport delay. Values of $G_{0,i}^{\min}$, $G_{0,i}^{\max}$ and $v_i^{\max}$ are given in Table 1 in the Appendix. Regarding the prediction horizon H_p, it has been established to be equal to 42 samples taking into account the worst-case transport delay/effect between the furthest gate and the control point.

5 Simulation Results

This section presents the main results obtained when HMPC is designed and tested by using the scheme presented in Figure 4. Simulation results have been obtained using the *clsSolve* solver of TOMLAB for MATLAB®, which implements the Fletcher-Xu hybrid method (modified Gauss-Newton BFGS algorithm) in a Dell Computer with Windows XP SP3 with Intel® Core™2 DUO P8400 2.2GHz and 1.95 Gb RAM. The maximum computation times for the considered scenarios are 19.5 s (first scenario) and 27.89 s. Both of them smaller than 100 s (sampling time used for control). This fact shows that the proposed controller is able to operate in real time. The optimisation problem has 126 decision variables and 756 constraints.

Figure 10 shows the results obtained in a first scenario corresponding to an input hydrogram with a flow-peak of 1000 m^3/s at the input of the system (inflow $q_{S_1}(k)$). This type of scenario occurs 1-3 times per year (0.37 years return period, 1927-2003). Figure 10(a) compares the input flow q_{S_1} against the outflow of the river reach S_7, namely q_{S_7}, where the performance of the predictive controller can be seen. The total amount of water stored in all the flooding zones is about 1.5 million of cubic meters in the most critical situation of flooding. The maximum

volume that can be stored at each flooding zone depends on the level of water in the river side since the flow towards/from flooding zones depends, in turn, on the level difference at both sides of the gates. For the considered flooding scenario, an upper bound of the maximum volume can be computed by considering each flooding zone independently and determining the maximum level of water at the river side when side gates are closed. Using this approach, the maximum volume that can be stored in the flooding zones is around three million of cubic meters. In this scenario, about 50% of this maximum volume is stored. This fact allows only to decrease the flow peak in about 20% the maximum flow (from $1000\,\mathrm{m}^3/\mathrm{s}$ to $800\,\mathrm{m}^3/\mathrm{s}$) at S_7 due to physical limitations. These physical limitations are related to the fact that flooding areas can only be filled by difference of levels between river and flooding areas and not by pumping (for example). When the level of the river reaches the same level as the flooding area, no more water can be stored in the flooding area.

Figure 10(b) shows the water level of the river and flooding zones and the side gate positions (control action) determined by the MPC controller. From this figure, it can be noted that the MPC controller does not open the side gate until it predicts that the flow will be higher than the maximum desirable flow, namely q_d, at S_7. At this point (approximately at time six hours and 40 minutes), the MPC controller opens the side gates to store water at the flooding zones in order to reduce the flow q_{S_7}. Gates have to be closed when their corresponding level at the river side is greater or equal to the level at the tank side (at time corresponding to ten hours and 50 minutes). Once the flow at S_7 is lower than q_d, the HMPC controller opens the side gates again for emptying the flooding zones. Finally, Figure 10(c) shows the amount of water stored and released corresponding to the three flooding zones.

Figure 11 presents the results when considering a two-peak inflow episode, each peak of $1000\,\mathrm{m}^3/\mathrm{s}$. In this scenario, the flooding zones stored more than two million of cubic meters (about 70% of the the volume that could have been stored by considering the maximum level of water in the river in front of the flooding zones when side gates are closed). Figure 11(a) shows that the peak reduction of q_{S_7} is about the same as in the latter case, i.e., about the 20%. In Figure 11(b) it can be noticed that the HMPC controller opens gates when the first peak arrives, closes gates between peaks to prevent emptying the flooding zones and opens them again when the second flow peak appears. Finally, once the flow in the control point is lower than q_d, gates are opened to empty the flooding zones. From Figure 11(c), it can be seen how water is stored during and between peaks in the flooding zones in order to reduce q_{S_7}.

A way to improve the results obtained in previous scenarios would consist in increasing the stored water of the flooding zones. This fact would imply to install an active system based on pumping stations in order to move water from/to the river to/from the flooding zones, rather than filling them *passively* from the difference between the river level and the considered flooding zone level.

6 Conclusions

In this paper, the problem of flooding control at the Ebro River in Spain is presented. The Ebro River presents flooding episodes in the city of Zaragoza in spring when snow melts in the Pyrenees. To avoid flooding in living areas, some lands outside the city are prepared to be flooded. This paper has presented a predictive control approach to manage induced flooding in pre-established areas by manipulating the side gates that regulate the water inflow to the land to be flooded. Several scenarios have been used to validate the performance of the proposed approach. Obtained results are promising to validate that flows at control points can be reduced. However, these results can be further improved by replacing the considered side gates by active

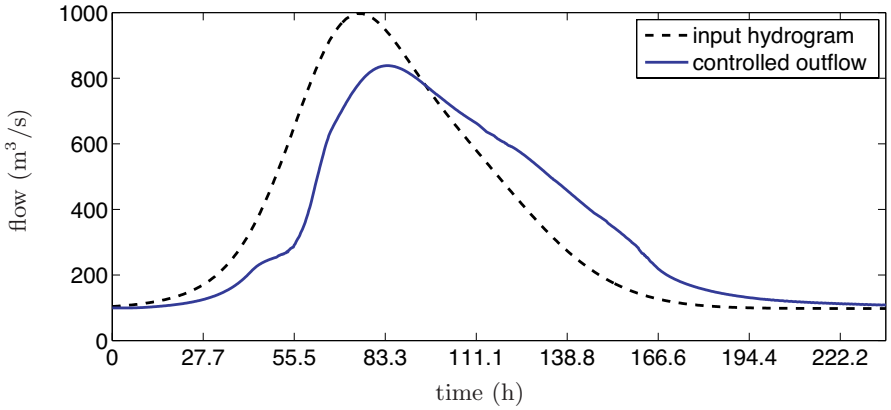

(a) Input and output flows

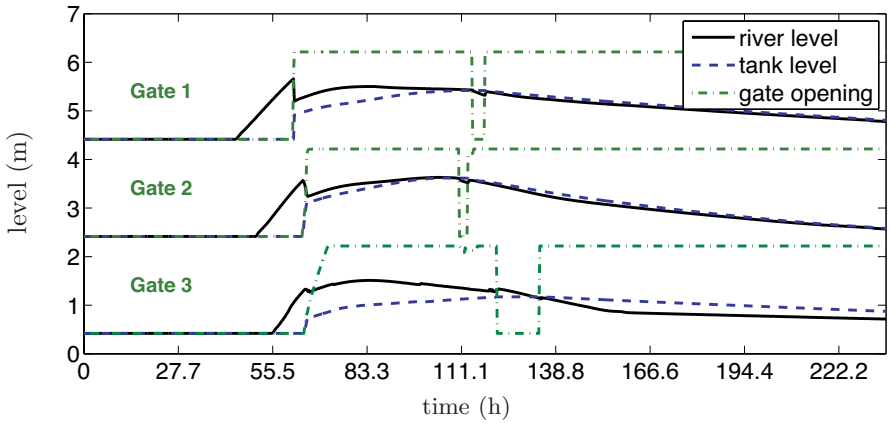

(b) Side gates movements and water levels

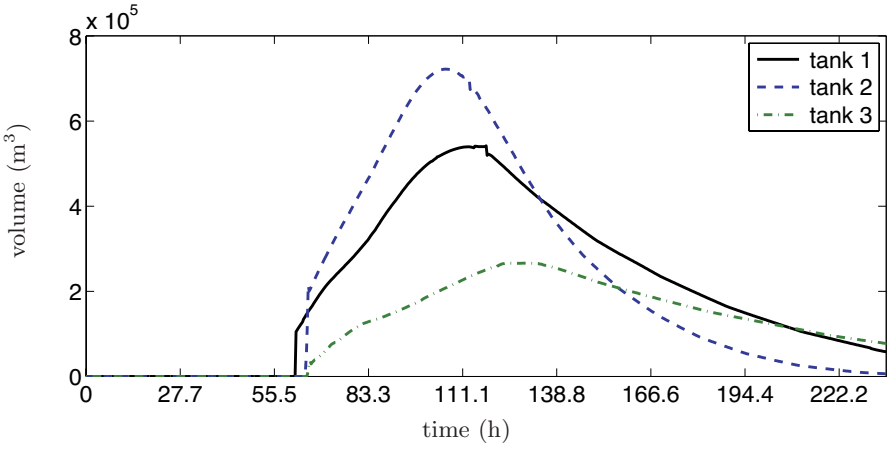

(c) Tank volumes

Figure 10: Results related to the first flooding scenario

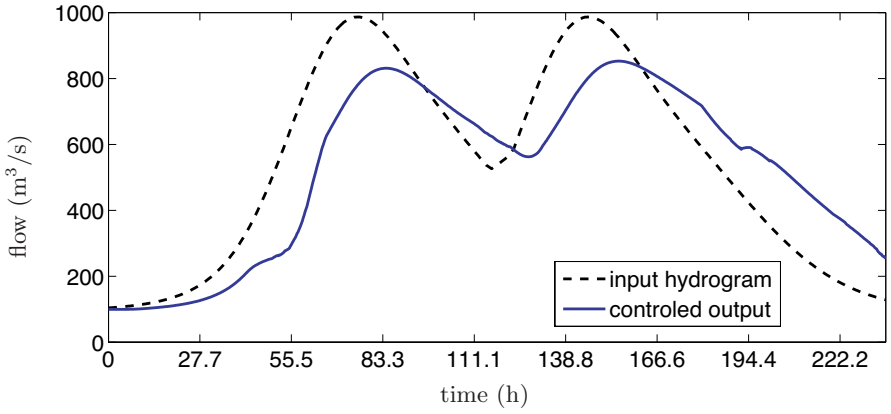

(a) Inflow and outflow

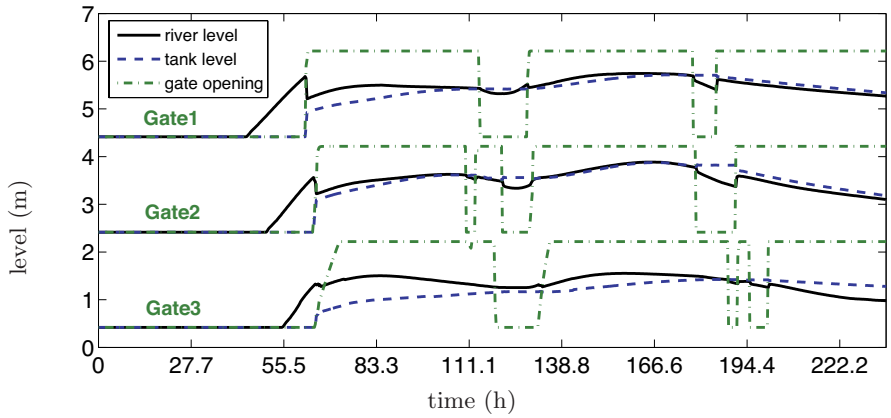

(b) Side gates movements and water levels

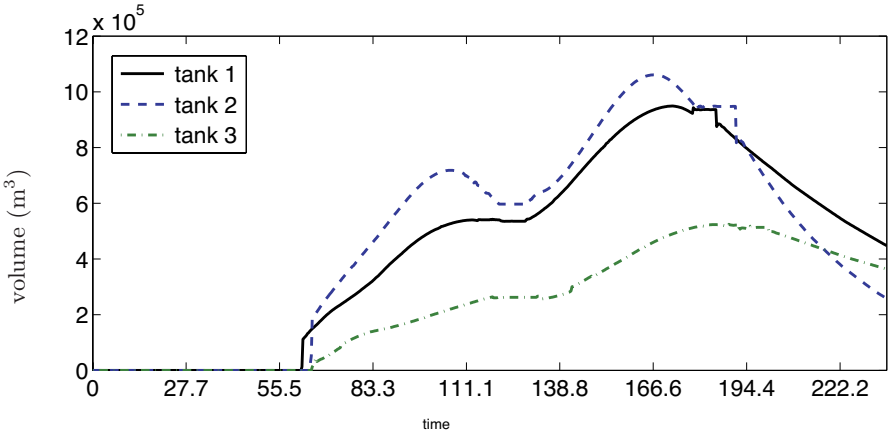

(c) Tank volumes

Figure 11: Results related to the second flooding scenario

mechanisms of water transport such as pumping stations to fill/empty the flooding zones.

Appendix

Table 1: Values for the case study parameters and coefficients

Parameter	Value $i=1$	Value $i=2$	Value $i=3$	Units
$z_{r,i}$	4.4	2.4	0.4	m
$z_{fz,i}$	4.4	2.4	0.4	m
$G_{0,i}^{\min}$	0	0	0	m
$G_{0,i}^{\max}$	8	8	8	m
ρ	30	30	30	m
K_1	3.330	3.330	3.330	–
K_2	2.248	2.248	2.248	–
$v_i^{\max}$	11313179.25	9748072.85	11142631.57	m^3
q_d		600		m^3/s
$a_{(2,i-1)}$	2.34	0.0103	-0.0000087	–
$a_{(4,i-1)}$	0.214	0.0111	-0.0000099	–
$a_{(6,i-1)}$	-1.88	0.0114	-0.0000105	–
$b_{(i,0)}$	67015136.2	11087504.69	318101.2	–
$b_{(i,1)}$	-45240197.55	-11755511.33	-1345357.23	–
$b_{(i,2)}$	11520399.05	4384007.67	1533165.62	–
$b_{(i,3)}$	-1397782.36	-713935.76	-381768.42	–
$b_{(i,4)}$	83583.67	56627.72	44799.9	–
$b_{(i,5)}$	-1972.08	-1753.99	-2000.71	–

Acknowledgements

This research has been partially founded by Generalitat de Catalunya project entitled *Gestión y control de zonas inundables para minimizar los impactos medioambientales de las crecidas de los ríos: Aplicación a la cuenca pirenaica* (GECOZI 2010CTP00043), the Spanish research project WATMAN (CICYT DPI2009-13744) of the Science and Innovation Ministry, and the DGR of Generalitat de Catalunya (SAC group Ref. 2009/SGR/1491). The authors thank Confederación Hidrográfica del Ebro for providing the case study used in this paper as well as for sharing their hydrological management expertise.

References

[1] M.B. Abbott and A.W. Minns. *Computational Hydraulics*. Ashgate Publishing Limited, England, 1998.

[2] A. Bemporad and M. Morari. Control of systems integrating logic, dynamics, and constraints. *Automatica*, 35(3):407–427, 1999.

[3] T. Barjas Blanco, P. Willems, P. Chiang, N. Haverbeke, J. Berlamont, and B. DeMoor. Flood regulation using non-linear model predictive control. *Control Engineering Practice*, 18(10):1147–1157, 2010.

[4] S. Boyd and L. Vandenberghe. *Convex Optimization*. Cambridge University Press, UK, 2004.

[5] M. Brdys and B. Ulanicki. *Operational Control of Water Systems: Structures, algorithms and applications*. Prentice Hall International, UK, 1994.

[6] J. Burguete and P. Garca-Navarro. Efficient construction of high-resolution tvd conservative schemes for equations with source terms: application to shallow water flows. *International Journal of Numerical Methods in Fluids*, 37:209–248, 2001.

[7] S. Domenech, F. Espejo, A. Ollero, and M. Snchez-Fabre. Recent floods in the middle ebro river, spain: hydrometeorological aspects and floodplain management. *Hydrology and Earth System Sciences Discussions*, 6:5937–5976, 2009.

[8] M. Gómez, J. Rodellar, and J.A. Mantecon. Predictive control method for decentralized operation of irrigation canals. *Applied Mathematical Modelling*, 26:1039 – 1056, 2002.

[9] B. Latorre, P. Garca-Navarro, J. Murillo, J. Burguete, G. Petaccia, B. Calvo, and F. Savi. Flood wave simulation with 1d-2d coupled models. In *Proceedings of Computing and Control in the Water Industry*, Sheffield , UK, September 2009.

[10] X. Litrico and V. Fromion. Simplified modeling of irrigation canals for controller design. *Journal of Irrigation and Drainage Engineering*, 130(5):373 – 383, 2004.

[11] X. Litrico and D. Georges. Robust continuous-time and discrete-time flow control of a dam-river system: (I) Modelling. *Applied Mathematical Modelling*, 23(11):809 – 827, 1999.

[12] X. Litrico and D. Georges. Robust continuous-time and discrete-time flow control of a dam-river system: (II) Controller design. *Applied Mathematical Modelling*, 23(11):829 – 846, 1999.

[13] L. Ljung. *System Identification: Theory for the User*. Prentice Hall, Englewood Cliffs, New Jersey, 1999.

[14] J.M. Maciejowski. *Predictive Control with Constraints*. Prentice Hall, Great Britain, 2002.

[15] C. Martin, C. M. Cardona, D. San Martin, A. Salterain, and E. Ayesa. Dynamic simulation of the water quality in rivers based on the IWA RWQM1: Application of the new simulator CalHidra 2.0 to the Tago river. *Water Science and Technology*, 54(11-12):75 – 83, 2006.

[16] J. Murillo, P. Garca-Navarro, J. Burguete, and P. Brufau. A conservative 2D model of inundation flow with solute transport over dry bed. *International Journal of Numerical Methods in Fluids*, 52:1059–1092, 2006.

[17] J. Murillo, P. Garcia-Navarro, J. Burguete, and P. Brufau. The influence of source terms on stability, accuracy and conservation in two-dimensional shallow flow simulation using triangular finite volumes. *International Journal for Numerical Methods in Fluids*, 54(5):543–590, 2007.

[18] C. Ocampo-Martinez. *Model Predictive Control of Wastewater Systems*. Advances in Industrial Control. Springer Verlag, 1 edition, 2011. ISBN: 978-1-84996-352-7.

[19] C. Ocampo-Martinez, A. Bemporad, A. Ingimundarson, and V. Puig. *Identification and Control: The Gap between Theory and Practice*, chapter On Hybrid Model Predictive Control of Sewer Networks, pages 87 – 114. Springer-Verlag, 2007.

[20] C. Ocampo-Martinez and V. Puig. Piece-wise linear functions-based model predictive control of large-scale sewage systems. *IET Control Theory & Applications*, 4(9):1581–1593, 2010.

[21] C. Ocampo-Martinez, V. V. Puig, and S. Bovo. Decentralised MPC based on a graph-partitioning approach applied to Barcelona drinking water network. In *Proceedings of the IFAC World Congress*, Milano (Italy), 2011.

[22] M. Schechter. Polyhedral functions and multiparametric linear programming. *Journal of Optimization Theory and Applications*, 53:269–280, 1987.

[23] R. Toro, C. Ocampo-Martinez, F. Logist, J. Van Impe, and V. Puig. Tuning of predictive controllers for drinking water networked systems. In *Proceedings of the IFAC World Congress*, Milano (Italy), 2011.

[24] P. J. van Overloop, S. Weijs, and S. Dijkstra. Multiple model predictive control on a drainage canal system. *Control Engineering Practice*, 16(5):531–540, 2008.

[25] E. Weyer. System identification of an open water channel. *Control Engineering Practice*, 9:1289 – 1299, 2001.